This is the peer reviewed version of the following article: F. Fanelli, S. Lovascio, R. d'Agostino, F. Fracassi, Insights into the Atmospheric Pressure Plasma-Enhanced Chemical Vapor Deposition of Thin Films from Methyldisiloxane Precursors, Plasma Process. Polym. 2012, 9, 1132–1143, which has been published in final form at https://doi.org/10.1002/ppap.201100157. This article may be used for non-commercial purposes in accordance with Wiley Terms and Conditions for Use of Self-Archived Versions. This article may not be enhanced, enriched or otherwise transformed into a derivative work, without express permission from Wiley or by statutory rights under applicable legislation. Copyright notices must not be removed, obscured or modified. The article must be linked to Wiley's version of record on Wiley Online Library and any embedding, framing or otherwise making available the article or pages thereof by third parties from platforms, services and websites other than Wiley Online Library must be prohibited.

Article type: Full Paper

Insights into the Atmospheric Pressure Plasma-Enhanced Chemical Vapor Deposition of Thin Films from Methyldisiloxane Precursors

Fiorenza Fanelli,* Sara Lovascio, Riccardo d'Agostino and Francesco Fracassi

---

Dr. F. Fanelli
CNR – Institute for Inorganic Methodologies and Plasmas (IMIP), c/o Department of Chemistry, University of Bari Aldo Moro–via Orabona 4, 70126 Bari, Italy
Dr. S. Lovascio, Prof. R. d'Agostino, Prof. F. Fracassi
Department of Chemistry, University of Bari Aldo Moro –IMIP CNR, via Orabona 4, 70126 Bari, Italy

---

This work describes the plasma-enhanced chemical vapor deposition of thin films at atmospheric pressure using dielectric barrier discharges fed with argon, oxygen and different methyldisiloxanes, i.e., hexamethyldisiloxane, pentamethyldisiloxane, and 1,1,3,3-tetramethyldisiloxane. The influence of the methyldisiloxane chemical structure and of the oxygen/methyldisiloxane feed ratio is investigated in order to provide insights into the organosilicon plasma chemistry at atmospheric pressure. As expected the FT-IR and XPS analyses show that the carbon content of the coatings depends on the number of methyl groups in the precursor molecule; in the case of coatings obtained with PMDSO and TMDSO carbon removal seems to be further enhanced by the presence of Si-H bonds. Gaschromatography-mass spectrometry analyses of the exhaust gas allows to assess the precursor depletion and to perform the quali-quantitative determination of by-products (e.g., silanes, siloxanes, silanols) formed by plasma activation. The results are exploited to rise hypotheses on the contribution of the different reaction pathways on the deposition mechanism.

Introduction

Over the last decades the plasma-enhanced chemical vapor deposition (PE-CVD) from organosilicon compounds, such as hexamethyldisiloxane (HMDSO) and tetraethoxysilane (TEOS), in mixture with oxidants (i.e., O_2 and N_2O), has attracted growing attention in the field of the surface processing of materials since it allows the production of a large variety of thin films with a chemical composition ranging from silicone-like to SiO_2-like. The low pressure PE-CVD is a well-established technology which allows to achieve an accurate control of coatings thickness, conformity, chemical composition and properties (e.g., dielectric constant, density, porosity, morphology, etc.).[1-9] A great deal of work has been produced to understand the basics of organosilicon-containing low pressure plasmas through different diagnostic investigations of both the deposits and the plasma phase. Important research tasks have been the identification of the reaction steps relevant for the deposition process and the correlation of the plasma chemistry with the stoichiometry, the structure and the final properties of the coatings (e.g., mechanical, electrical, optical and gases/moisture diffusion properties). Therefore, the proposed deposition mechanism [10,11] rationalizes the published experimental evidences, i.e., the effect of process parameters, such as feed composition, power density, substrate temperature, substrate bias voltage, etc..

Recently the interest of both academic and industrial community has been expanded to the employment of atmospheric pressure plasma technologies due to the potential reduction of process costs and to the easier inline integration with respect to low pressure plasmas. Among the different approaches to generate cold plasmas at atmospheric pressure, dielectric barrier discharges (DBDs),[13,14] both in filamentary and homogeneous regime, have been addressed as an attractive route towards the production of thin films and, over the last few years, many investigations have been published in particular on the PE-CVD form organosilicon-containing feeds. As in low pressure plasmas, HMDSO is one of the most widely used

organosilicon precursors[15-26] due to its non-toxic character, chemical inertness, and relatively high vapor pressure even at room temperature, however several studies propose the utilization of other compounds such as tetraethoxysilane,[15,21] hexamethyldisilazane,[16,27] tetramethylcyclotetrasiloxane,[28] octamethylcyclotetrasiloxane,[28] etc..

The most critical feature of DBDs, which often complicates the utilization in surface processing of materials, is their possible operation under completely different discharge regimes: filamentary and homogeneous regimes.[13,14] The filamentary DBDs (FDBD), in spite of the easy generation, are intrinsically inhomogeneos discharges formed by several short-living and narrow microdischarges which in some cases can lead to non-uniform and damaged coatings;[13,14] on the other hand the homogeneous DBDs (i.e., glow or Townsend discharges), more suitable for uniform surface treatment, are generally characterized by a quite narrow operational window.[13,14]

Published studies on organosilicon-containing DBDs first of all clearly demonstrated the possibility of tuning the chemical composition of the coatings by simply changing the oxidant concentration in the feed.[15,17,23-25,27] Massines et al.,[17] working with homogeneous discharges fed with N_2-HMDSO-N_2O mixtures, investigated the chemical composition of the deposits by changing the N_2O/HMDSO ratio. Dense SiO_2-like coatings, with negligible carbon and nitrogen content but detectable silanol (Si-OH) groups,[17] were obtained at N_2O/HMDSO ratio greater than 6.

The deposition of SiO_2-like layers on large area polymeric substrates was performed in a roll-to-roll reactor by means of homogeneous DBDs[19-21] fed by different mixtures such as Ar-N_2-O_2-HMDSO[20,21] and Air-Ar-HMDSO.[21] The possibility of obtaining the homogeneous regime for a wide range of plasma parameters and feed gas mixtures was demonstrated. The deposited SiO_x layers were characterized by a high quality in terms of adhesion to the substrate, smoothness, uniformity, purity, packing density and low level of surface defects comparable to the uncoated polymer.[20,21] It was also shown that the formation of powders,

detrimental for the quality of the deposit, can be avoided by using a pulsed power supply and adequate gas residence time in the discharge zone.[29] On the other hand, in the case of a filamentary DBD, Boscher et al.[25] demonstrated that the employment of a pulsed power supply enhances the film homogeneity also on metallic substrates, allowing the growth of pinhole-free films.

Nowadays, besides the continuous improvements in atmospheric pressure deposition performances, there is an urgent demand to investigate the plasma chemistry with the aim of gaining insights into the deposition mechanisms. The research should be addressed to detect the film precursors, to identify the main reaction pathways (both homogeneous and heterogeneous processes) and to clarify the plasma-surface interaction. The comparison between different reactive systems, namely the investigation of various organosilicon precursors, as well as the utilization of different diagnostic techniques of the plasma phase could definitely lead to the understanding of the atmospheric pressure plasma processes.

Among the few published studies concerning the chemistry of organosilicon-containing atmospheric pressure plasmas, the FT-IRAS (Fourier transform infrared absorption spectroscopy) investigation of HMDSO-fed DBDs, allowed Vinogradov et al.[24] to suggest that HMDSO fragmentation mainly produces four fragment, $(CH_3)_3SiO$, $Si(CH_3)_3$, $(CH_3)_3SiOSi(CH_3)_2$ and CH_3, which can be responsible of pentamethyldisiloxane, trimethylsilane and methane formation. The concentration of these species, as well as of the precursor, decreases with O_2 addition to the feed for oxidation processes with consequent formation of CO, CO_2, H_2CO, O_3 and $HCOOH$.

GC-MS was utilized by Sonnenfeld et al.[15] to investigate the exhaust gas of HMDSO-contaning atmospheric pressure cold plasmas. In particular, in the case of an Ar-HMDSO-O_2 fed ferroelectric barrier discharge the only identified by-products were pentamethyldisiloxane, trimethylsilane, tetramethylsilane, and some low molecular weight hydrocarbons. O_2 addition did not result in the appearance of oxidation products. Since only small amounts of

unidentified oligomerization products (i.e., species heavier than HMDSO) were detected, the authors assumed that the polymerization process mainly takes place at the surface of the growing polymer.

Recently we reported preliminary results on the GC-MS investigation of the exhaust gas of filamentary DBDs fed by Ar in mixture with oxygen and different methyldisiloxanes.[14,26,30] In particular we investigated in detail the PE-CVD with Ar-HMDSO-O_2 mixtures by comparing the FT-IR spectra of the deposited coatings with the GC-MS analyses of the exhaust gas.[26] Without O_2 addition to the feed a coating with high monomer structure retention is obtained and the exhaust contains several by-products such as silanes, silanols, and linear and cyclic siloxanes. O_2 addition does not enhance the activation of the monomer while it highly influences the chemical composition and structure of the deposited coating as well as the quali-quantitative distribution of by-products in the exhaust gas.

In this work we report our recent results on the deposition of thin films in atmospheric pressure DBDs fed by argon in mixture with oxygen and different methyldisiloxanes (MDSO), i.e., hexamethyldisiloxane (HMDSO), pentamethyldisiloxane (PMDSO) and 1,1,3,3-tetramethyldisiloxane (TMDSO). The molecular structure of the three precursors differs in the number of methyl groups (i.e., HMDSO > PMDSO > TMDSO), and in the number of Si-H bonds (i.e., HMDSO < PMDSO < TMDSO). The effect of the feed composition, in terms of chemical structure of the organosilicon precursor and of oxygen-to-methyldisiloxane feed ratio, on the properties of the deposits as well as on monomer depletion and on by-products concentration, was investigated with the aim of developing hypotheses on the main reaction pathways of the overall deposition mechanism.

Experimental Section

PE-CVD

The atmospheric plasma was generated between two parallel plate electrodes (2 mm gap, 50×50 mm^2 electrode area), both covered with an Al_2O_3 plate (CoorsTek, purity of 96%, thickness of 2.54 mm), by applying an AC high voltage (7 kV_{p-p}) at 30 kHz by means of a STT Calvatron power supply (model SG2).[26] The electrode system was located into a Plexiglas chamber (volume of about 14 L) slightly pumped with a dry diaphragm pump (Pfeiffer) to keep the working pressure constant (10^5 Pa) as measured by a MKS baratron (**Figure 1**).

Experiments were performed by keeping constant the Ar and organosilicon precursor flow rates at 4000 sccm and 1 sccm, respectively and changing the O_2 flow rate in order to vary the O_2/MDSO feed ratio in the range 0 – 40. The gas flow rates were controlled with MKS mass flow controllers; the vapors of the organosilicon precursor (HMDSO: Fluka 98.5% purity, PMDSO: ABCR 99% purity, TMDSO: ABCR 99% purity) were introduced into the reactor by an Ar stream bubbling through a liquid reservoir kept at 30°C. The effective amount of precursor admitted into the reactor was evaluated by weight variation per unit time of the reservoir and, assuming an ideal gas behavior, it was converted into flow rate expressed in sccm. The feed gas was introduced in the discharge zone through a slit and pumped through a second slit positioned on the opposite side (longitudinal gas injection).[26] Under these conditions the gas residence time in the interelectrode zone was equal to about 80 ms. Before each experiment, the Plexiglas chamber was purged with 4000 sccm of Ar for 20 min to remove air contaminations. The deposition processes were carried out for 5 min.

DBD electrical characterization

The voltage applied to the electrodes was measured by means of a high voltage (HV) probe (Tektronix P6015A, 75 MHz bandwidth, 1000 attenuation factor). The current (I) and the charge (Q) were evaluated by measuring with a Tektronix P2200 probe the voltage drop across a 50 Ω resistor and a 4.7 nF capacitor connected in series with the grounded electrode, respectively. The data were recorded by means of a digital oscilloscope (Tektronix TDS2014B). The power dissipated in the discharge was evaluated employing the Manley method and in particular the voltage-charge (V-Q) Lissajous figure.[26] The dissipated power was expressed as specific power per unit of electrode surface.

Film characterization

The chemical structure of the deposited thin films was investigated by means of Fourier transform infrared spectroscopy (FT-IR). A commercial Brucker Equinox 55 FT-IR interferometer was used to collect the infrared absorption spectra (400 - 4000 cm^{-1} range, 4 cm^{-1} resolution) of the films deposited onto 0.7 mm thick c-Si(100) substrates. In order to minimize the effects of carbon dioxide and water vapor, the optical path inside the sample compartment was purged with nitrogen for 10 min between each measurement. After baseline correction, spectra were normalized to the most intense absorption band (Si-O-Si).

Atomic composition of the films was determined by X-ray photoelectron spectroscopy (XPS) using a Theta Probe spectrometer (Thermo VG Scientific) equipped with a monochromatic Al K_α X-ray source (1486.6 eV) operated at a spot size of 400 μm corresponding to a power of 100 W. Survey (0–1200 eV) and high resolution (Si2p, C1s, and O1s) spectra were recorded at a pass energy of 200 eV and 150 eV, respectively. All spectra were acquired at a take-off angle of 37° with respect to the sample surface. A flood gun was used to balance the surface charging. In order to remove carbon contamination from the sample surface, 10 s sputter cleaning with 1 keV and 500 nA Ar^+ ions was carried out before the analysis.

Film thickness was evaluated on substrates partially masked during the deposition using an Alpha-Step 500 KLA Tencor Surface profilometer. Surface morphology was investigated by means of scanning electron microscopy (SEM) using a digital microscope EVO 40XVP (Zeiss); the samples analysed by SEM were coated with a thin film of gold (thickness of 50 nm).

In order to compare the results obtained under different experimental conditions, film thickness measurements, FT-IR, XPS and SEM analyses were carried out on films deposited in the middle of the interelectrode region, that is in the region 20-30 mm from the gas entrance inside the discharge area.[26] FT-IR analyses were also performed on samples positioned downstream of the electrode area (50 - 60 mm from the gas entrance inside the discharge area).[26]

Exhaust gas sampling and analysis

A stainless steel liquid nitrogen trap, located between the reactor and the pump (Figure 1), was employed to sample the stable species contained in the exhaust gas.[11,26] Sampling was performed for 30 min, then the trap was isolated from the system, the condensate was dissolved in acetone (Sigma-Aldrich, 99.8% purity) and the solution was filtered and analyzed by means of gaschromatography (GC) with mass spectrometric (MS) detection. The GC apparatus (GC 8000Top Thermoquest Corporation) was equipped with a Grace AT™-1MS fused silica capillary column (polydimethylsiloxane 0.25 μm thick stationary phase, length of 30 m, internal diameter of 0.25 mm). The analyses were performed with 1 sccm of He as carrier gas, at 200°C injector temperature and a column temperature programmed from 30 to 200°C (temperature program: 1 min at 30°C, linear heating rate of $10°C{\cdot}min^{-1}$, 1 min at 200°C). Separated products were analyzed with a quadrupole mass spectrometer (Voyager, Finnigan, Thermoquest Corporation) at the interface and source temperature of 250 and 200°C, respectively. Mass spectra were recorded in full-scan mode in the m/z range 15–500 at

the standard ionizing electron energy of 70 eV. The products were identified by means of available libraries,[31] some species were tentatively identified through the interpretation of their mass spectra according to the typical fragmentations pattern of organosilicon compounds. The identification of some products was confirmed by the comparison of retention time and mass spectrum with standard compounds. The quantitative analysis of some identified products was performed utilizing nonane (Sigma Aldrich, 99% purity) as internal standard (IS) through calibration curves in the linear range, utilizing the area of the corresponding peaks in the chromatogram acquired in full-scan mode. The amounts of quantified compounds were then expressed as a flow rate.[26] The extent of organosilicon precursor utilized by the plasma process, namely the MDSO depletion ($MDSO_{depletion}$), is calculated according to equation (1):

$$MDSO_{depletion} = \frac{\Phi_{MDSO\ OFF} - \Phi_{MDSO\ ON}}{\Phi_{MDSO\ OFF}} \cdot 100 \qquad (1)$$

where $\Phi_{MDSO\ OFF}$ and $\Phi_{MDSO\ ON}$ are the monomer flow rates in the gaseous effluent in plasma off and plasma on conditions, respectively. Considering the overall analytical procedure (sampling, manipulations, and GC-MS analysis) the limit of quantification (LOQ) of by-products in the exhaust was approximately 10^{-4} sccm. The LOQ corresponds to by-product amount resulting in an intensity of the chromatographic peak greater than 10 times the standard deviation of the blank signal.[32]

Results and Discussion

DBD characterization

Under the experimental conditions explored in this work filamentary DBDs are obtained. Whatever the methyldisiloxane, the current signals contain several peaks characteristic of filamentary discharges.[14,26] In particular at O_2/MDSO feed ratio of 0 the discharge current is formed by a quasi-periodical multipeak signal and the filamentary discharge is characterized by a quasi-homogeneous appearance ascribed to stochastically distributed microdischarges; under this condition only few filaments were observed in the gas gap with the naked eye. The filamentary character increases with oxygen addition to the gas feed because the number of current peaks increases within each half-cycle, and at O_2/MDSO feed ratios greater than 6 the DBD exhibits numerous, intense and well-distinguished filaments.[26] With increasing the O_2/MDSO feed ratio from 0 to 40 the average specific discharge power increased from about 0.20 to 0.33 $W \cdot cm^{-2}$.

Film characterization

Film morphology was investigated by SEM (**Figure 2**) for O_2/MDSO feed ratios higher than 1, since without oxygen addition an oily coating can be obtained in particular with HMDSO. Figures 2a-2b show that smooth and powder-free coatings are obtained with HMDSO even at oxygen-to-monomer ratio of 25 (powders start to be detected on the deposit surface at values of the ratio higher than 40). With PMDSO powders appear at O_2/PMDSO feed ratio of 25 (Figure 2e), while with TMDSO powder formation is evident also with low oxygen content in the feed. As shown by Figure 2g, it seems that the deposition process of TMDSO is dominated by the formation of high molecular weight oligomers which at low O_2/TMDSO ratios are included in the deposit in the form of globules. The higher tendency of PMDSO and principally TMDSO to form powders affects the characteristics of the deposits collected

downstream the electrode region. With HMDSO (Figure 2c) a coating with incorporated powders is obtained, while with PMDSO and TMDSO unadherent deposits of agglomerated nanoparticles are obtained (Figures 2f and 2i).

The chemical structure of the films deposited without O_2 addition depends on the organosilicon precursor utilized. As shown by the FT-IR spectra reported in **Figure 3**, the intensity of the IR absorptions of carbon-containing groups (e.g., CH_x and $Si(CH_3)_x$ at 2850-3000 cm^{-1} and about 1258 cm^{-1}, respectively)[1,2,5,7-9,26] are higher for HMDSO which has two methyl groups more than TMDSO. At a O_2/MDSO feed ratio of 1 these absorptions almost completely disappear in the case of TMDSO, while they are still well visible for the other two monomers that require a higher stoichiometric amount of O_2 for the complete oxidation. This can be better appreciated in **Figure 4**, where the FT-IR absorption integral ratio $Si(CH_3)_x$/SiOSi is plotted vs. the O_2/MDSO feed ratio. The integral ratio is scaled in the order HMDSO > PMDSO > TMDSO. A similar trend is observed also for the FT-IR absorption integrals ratio CH_x/SiOSi.

The increase of the O_2 content in the feed also results in the appearance of silanol absorptions (namely the broad OH absorption in the 3200 – 3600 cm^{-1} region and the Si-OH stretching at 905 cm^{-1}) as well as in the shift of the intense Si-O-Si asymmetric stretching band from about 1040 cm^{-1} to higher wavenumbers.[1,2,5,7-9,26] At the O_2/HMDSO feed ratio of 25, the asymmetric stretching of Si-O-Si falls at 1050 cm^{-1} for the residual presence of carbon-containing groups, while for O_2/PMDSO and O_2/TMDSO the peak shifts to 1070 cm^{-1}, as for inorganic SiO_2-like coatings.[1,2,5,8,9] In agreement with FT-IR, the XPS results of **Figure 5**a clearly show that the decrease of the carbon content of the coatings with oxygen addition to the feed is steeper for PMDSO and TMDSO rather than for HMDSO. Moreover the XPS O/Si ratio (Figure 5b) is 2 - 2.1 for PMDSO and TMDSO at the MDSO/O_2 feed ratio as low as 6, while for HMDSO at feed ratios of 40. The slightly over-stoichiometric amount of oxygen in

the SiO_x coatings is consistent with the presence of the appreciable amount of silanol groups,[17,20] detected by FT-IR.

The deposition rate in HMDSO containing plasma slightly decrease in the 120-150 nm min^{-1} range with oxygen addition (Figure 5c), while in the case of the other two organosilicons shows a marked decrease. The lowest deposition rate is registered for TMDSO (25 nm min^{-1}) at O_2/TMDSO feed ratio higher of 6.

The FT-IR spectra of the coatings deposited inside the discharge zone and of the powders/coating collected downstream the electrode region at the O_2/MDSO feed ratio of 25 are compared in **Figure 6**. The downstream powders show higher absorptions of CH_x and Si-$(CH_3)_x$ groups and a broader Si-O-Si asymmetric stretching due to the marked increase of the shoulder at about 1120 cm^{-1}, that could be related to a less dense and disordered network with respect to the deposit in the discharge zone.[9,26] It is worth mentioning that without oxygen addition to the feed, the FT-IR spectra of the deposit collected in the discharge and downstream are very similar. As already hypothesized,[26] the lower organic character of the film deposited inside the discharge with oxygen addition suggests that part of the oxidation reactions occurs on the surface of the growing film in the discharge (i.e. heterogeneous oxidation). A quite similar carbon content should be expected both inside the discharge and downstream if heterogeneous oxidation was not important in the DBD.

The different reactivity of the three methyldisiloxanes can be better clarified by comparing the FTIR of the coating deposited at the O_2/MDSO feed ratios of 12, 10.5 and 9 for HMDSO, PMDSO and TMDSO, respectively, which correspond to the stoichiometric ratios for the theoretical complete oxidation of the three methyldisiloxanes. FT-IR absorptions of the carbon-containing groups increase in the order TMDSO < PMDSO < HMDSO (**Figure 7**), while XPS analyses show a carbon atomic concentration much higher for HMDSO (30%) than for PMDSO (5%) and TMDSO (4%). This evidence allows to claim that the removal efficiency of the carbon-containing moieties observed for the three methyldisiloxanes can be

ascribed to the enhanced reactivity of PMDSO and TMDSO due the presence of Si-H bonds. In fact, if the differences between the reactivity of the three compounds were mainly due to the different number of methyl groups in the organosilicon molecule, a quite similar carbon content should be observed for the coatings obtained at the O_2/MDSO feed ratio equal to the stoichiometric ratio of the complete oxidation reaction of the three methyldisiloxanes.

Exhaust gas investigation

The GC-MS investigation of the exhaust gas allowed to assess the percentage of unreacted organosilicon precursor and, therefore, its depletion (i.e., the amount of the organosilicon precursor transformed by the DBD). **Figure 8**a shows that the MDSOs depletion is not complete and it is not enhanced by oxygen addition to the feed gas. In the case of HMDSO a depletion reduction from 76 to 50% is registered in the O_2/HMDSO ratio range investigated in this work (0 – 40), while for PMDSO and TMDSO the depletion variation with oxygen addition is negligible. Although the rationalization of these results is not easy, it can be concluded that, under the experimental conditions utilized, the oxygen affects the chemical composition of the deposits but does not play a fundamental role in precursor activation (i.e., in the first step of the overall reaction). Moreover figure 8a shows that the number of methyl groups or Si-H bonds does not influence the MDSO depletion and hence the precursor activation.

The identified by-products formed in HMDSO-, PMDSO- and TMDSO-containing DBDs are reported in **Table 1**. It can be appreciated that the methyldisiloxane precursors form many different linear and cyclic compounds containing up to five silicon atoms. Among them some silanes (e.g., trimethylsilane and tetramethylsilane) are identified, indicating the dissociation of the Si-O bond of the precursor molecule and the formation of new bonds (Si-H and Si-C bond, respectively). Other species could be formed from the dissociation of the Si-H and Si-C bond of the precursor molecule (e.g., HMDSO in PMDSO-containing DBDs, PMDSO in

HMDSO-containing DBDs, etc). Linear and cyclic methyldisiloxanes with the general formula $SiMe_3$-$(Me_2SiO)_n$-$SiMe_3$ (n = 1–4) and $(Me_2SiO)_n$ (n = 3–4) are also formed for the occurrence of oligomerization and ring formation reactions. Some species contain also the –MeHSiO– units (e.g., heptamenthyltrisiloxanes, 1,1,3,3,5,5-hexamthyldisiloxane). Some compounds, such as the 2,2,4,4,5,5,7,7-octamethyl-3,6-dioxa-2,4,5,7-tetrasilaoctane and the 2,2,4,4,5,5,7-heptamethyl-3,6-dioxa-2,4,5,7-tetrasilaoctane, give evidence of the formation of Si-Si bonds. Finally compounds containing the silanol group (i.e., trimethylsilanol and hydroxypentamethyldisiloxane) are also revealed. Quite similar species were detected in the exhaust gas of low pressure of HMDSO-fed glow discharges.[11]

Figure 9 outlines possible pathways which could lead to the formation of some identified by-products in HMDSO-containing DBDs after cleavage of the Si-O and Si-C bonds in the precursor molecule.

The number and concentration of heavy oligomers (containing from 3 to 5 silicon atoms) decreases in the order HMDSO > PMDSO > TMDSO (i.e., with decreasing the number of methyl groups in the precursor molecule). As an example pentasiloxanes and tetrasiloxanes are observed only with HMDSO, trisiloxanes are detected both with HMDSO and PMDSO, while 1,1,3,3,5,5-hexamethyltrisiloxane is the sole compound containing more than 2 silicon atoms detected in the exhaust gas of TMDSO-containing DBDs. The almost complete absence of oligomerization by-products detected for TMDSO, also without O_2 addition (Table 1), is in agreement with globules formation observed by SEM analyses (Figure 2g). It seem to be reasonable to assume in fact that, due to the high reactivity of the fragments formed by the TMDSO activation, the reactions of oligomerization are mainly pushed towards the production of high molecular weight compounds which are included in the deposited coating in form of globules.

Oxygen addition results in the steep decrease of the concentration of most silanes and siloxanes below the quantification limit likely due to total oxidation reactions leading finally

to CO, CO_2 and H_2O (see for instance the octamethyltrisiloxane flow rate in Figure 8b). This trend is well correlated with the variation of the chemical composition of the deposited film provoked by oxygen addition to the feed (Figure 3 and 4).

A different behavior is observed for silanols. Figures 8c and 8d show that in HMDSO-containing DBDs the flow rate of both the trimethylsilanol and hydroxypentamethyldisiloxane decreases with increasing the O_2/HMDSO ratio, but it is never below the quantification limit. By comparing these trends with the FT-IR spectra of the deposits (Figure 3) it can be observed that, at high O_2/HMDSO feed ratios, the amount of Si-OH groups in the film is high while the silanol content in the exhaust is very low; therefore, it is possible to rise the hypothesis that the formation of Si-OH groups present in the coatings could mainly occur on the film surface through heterogeneous reactions, and not in the gas phase.[26,30] On the other hand, the reduction of the silanols content with oxygen addition in Figures 8c and 8d could be due to their more efficient inclusion in the growing film with consequent decrease of their gas phase concentration. However in this case an important variation of the sticking coefficient of the silanols on the surface of the growing film should be assumed as a function of gas feed composition; this variation is unlikely to occur for the high reactivity of silanols, which should be always characterized by high sticking coefficient.

The increase with O_2 concentration of hydroxypentamethyldisiloxane in PMDSO-containing DBDs (Figure 8d) is likely due to the reaction of the Si-H bond of the PMDSO molecule.

Discussion

The results presented in this work support the general deposition mechanism already reported for the low pressure PE-CVD[11] and described in **Figure 10**. According to this overall mechanism, the first reaction step (S1) is the activation of the organosilicon precursor by electron collision and/or reaction with excited Ar to produce the primary reactive fragments. Since under the experimental condition utilized in this study monomer depletion is not

increased by oxygen addition (see Fig 8a) the contribution to monomer activation of reactions with oxygen atoms or excited oxygen molecules is unlikely. Primary and secondary fragments can undergo heterogeneous gas-surface reactions, which contribute to film growth (S2), and homogeneous reactions such as oligomerization (S3) that can ultimately lead to powder formation (S4). The primary fragments can also undergo gas phase homogeneous oxidation to form partially (S5) and totally oxidized secondary (S6) fragments. Oligomers and partially oxidized fragments can also contribute to the film growth (S7 and S8), while powders can deposit both in the discharge and in the downstream zone (S9). The oxidation of the deposit is completed by the heterogeneous gas-surface reaction due to oxygen atoms or molecules with release of water and other oxidized volatile compounds (S10). The lower organic character of the film deposited inside the discharge, with respect to the powder collected downstream of the electrode region, indicates that the heterogeneous gas-surface oxidation inside the plasma plays a key role.

The relative importance of the different reactive steps in the overall mechanism is different for the organosilicon precursor under investigation:

(i) After activation (i.e., the first reaction step S1), PMDSO and TMDSO, are characterized by higher reactivity than HMDSO, resulting in a more efficient reduction of the carbon content of the deposits;

(ii) With TMDSO the production of heavy oligomers and powders is very important since they are included in the deposit in form of globules even without oxygen addition to the feed.

(iii) In the case of HMDSO the silanols present in the deposit could be essentially due to heterogeneous gas-surface reactions, while for PMDSO the incorporation of silanols present in the plasma phase cannot be ruled out due to the trend of hydroxypentamethyldisiloxane.

These considerations allow to conclude that the relative importance of each reaction step can be quite different even for similar compounds under similar experimental conditions and, therefore, any generalization cannot be safely done.

Conclusion

The deposition of thin film in atmospheric pressure plasma was studied in FDBDs fed with argon, oxygen and three different methyldisiloxanes in order to investigate the influence of the organosilicon precursor chemical structure on the deposition process.

As expected, the chemical composition of the coatings is strictly dependent on the oxygen content in the feed. Whatever the organosilicon precursor, it was possible to move from silicone-like to SiO_2-like thin films by increasing the O_2/MDSO feed ratio. However the reduction of the carbon content of the deposits with oxygen addition is scaled in the order TMDSO > PMDSO > HMDSO. Some evidences induce to claim that the process efficiency in removing the carbon content of the coatings is not simply related to the number of methyl groups in the precursor molecule, but it is enhanced by the presence of reactive Si-H bonds.

The GC-MS investigation of the exhaust gas allowed to assess that O_2 addition does not enhance the precursor depletion, while promotes a steep decrease of the concentration of silanes and siloxanes below the quantification limit. A different behavior is observed for silanols: their concentration in the exhaust is never below the quantification limit in the case of HMDSO- and PMDSO-containing DBDs. Silanols groups contained in the deposits obtained from HMDSO-fed DBDs are more likely formed through heterogeneous (plasma-surface) reactions; while in the case of PMDSO-containing DBDs the possible incorporation of silanols formed in the gas phase can not be excluded.

Considering the overall deposition mechanism, the results obtained in this work highlight that the relative importance of each reaction step can be quite different even for similar compounds under similar experimental conditions.

Acknowledgements: This research has been financially supported by Regione Puglia ("Accordo di programma quadro ricerca scientifica, II atto integrativo", project n. 51 "LIPP"). Piera Bosso is acknowledged for the scientific collaboration.

Received: ((will be filled in by the editorial staff)); Revised: ((will be filled in by the editorial staff)); Published online: ((please add journal code and manuscript number, e.g., DOI: 10.1002/ppap.201100001))

Keywords: atmospheric pressure cold plasma; dielectric barrier discharge; methyldisiloxane; PE-CVD.

[1] A. M. Wróbel, M. Wertheimer, in *Plasma Deposition, Treatment, and Etching of Polymers*, (Ed.: R. d'Agostino), Academic Press, New York **1990**, p. 163.

[2] F. Fracassi, R. d'Agostino, P. Favia, *J. Electrochem. Soc.* **1992**, *139*, 2636.

[3] P. Favia, R. d'Agostino, F. Fracassi, *Pure Appl. Chem*. **1994**, *66*, 1373.

[4] D. Hegemann, U. Vohrer, C. Oehr, R. Riedel, *Surf. Coat. Technol.* **1999**, *116–119*, 1033.

[5] G. Borvon, A. Goullet, A. Granier, G. Turban, *Plasmas Polym.* **2002**, *7*, 241.

[6] L. Zajíčková, V. Buršíková, J. Janča, *Vacuum* **1998**, *50*, 19.

[7] A. Grill, *J. Appl. Phys.* **2003**, *93*, 1785.

[8] T. B. Casserly, K. K. Gleason, *Plasma Process. Polym.* **2005**, *2*, 679.

[9] A. Milella, J. L. Delattre, F. Palumbo, F. Fracassi, R. d'Agostino, *J. Electrochem. Soc.* **2006**, *153*, F106.

[10] D. Magni, Ch. Deschenaux, Ch. Hollestein, A. Creatore, P. Fayet, *J. Phys. D: Appl. Phys.* **2001**, *34*, 87.

[11] F. Fracassi, R. d'Agostino, F. Fanelli, A. Fornelli, F. Palumbo, *Plasmas Polym.* **2003**, *8*, 259.

[12] D. S. Wavhal, J. Zhang, M. L. Steen, E. R. Fisher, *Plasma Process. Polym.* **2006**, *3*, 276.

[13] S. E. Alexandrov, M. L. Hitchman, *Chem. Vap. Deposition* **2005**, *11*, 457.

[14] F. Fanelli, *Surf. Coat. Technol.* **2010**, *205*, 1536.

[15] A. Sonnenfeld; T. M. Tun, L. Zajickova, K. V. Kozlov, H.-E. Wagner, J. F. Behenke, R. Hippler, *Plasmas Polym.* **2001**, *6*, 237.

[16] D. Trunec, Z. Navratil, P. Stahel, L. Zajickova, V. Bursikova, J. Cech, *J. Phys. D: Appl. Phys.* **2004**, *37*, 2112.

[17] F. Massines, N. Gherardi, A. Fornelli S. Martin, *Surf. Coat. Technol.* **2005**, *200*,1855.

[18] H. Caquineau, I. Enache, N. Gherardi, N. Naudé, F. Massines, *J. Phys. D: Appl. Phys.* **2009**, *42*, 125201.

[19] S. A. Starostin, P. A. Premkumar, M. Creatore, E. M. van Veldhuizen, H. de Vries, R. M. J. Paffen, M. C. M. Van de Sanden, *Plasma Sources Sci. Technol*. **2009**, *18*, 045021.

[20] P. A. Premkumar, S. A. Starostin, H. de Vries, R. M. J. Paffen, M. Creatore, T. J. Eijkemans, P. M. Koenraad, M. C. M. van de Sanden, *Plasma Process. Polym*. **2009**, *6*, 693.

[21] P. A. Premkumar, S. A. Starostin, M. Creatore, H. de Vries, R. M. J. Paffen, P. M. Koenraad, M. C. M. Van de Sanden, *Plasma Process. Polym.* **2010**, *7*, 635.

[22] B. Twomey, M. Rahman, G. Byrne, A. Hynes, L.-A. O'Hare, L. O'Neill, D. Dowling, *Plasma Processes Polym.* **2008**, *5*, 737.

[23] R. Morent, N. De Geyter, S. Van Vlierberghe, P. Dubruel, C. Leys, E. Schacht, *Surf. Coat. Technol.* **2009**, *203*, 1366.

[24] I. Vinogradov, D. Zimmer, A. Lunk, *Plasma Process. Polym.* **2009**, *6*, S514.

[25] N. D. Boscher, P. K. Choquet, D. Duday, S. Verdier, *Plasma Process. Polym.* **2010**, *7*, 163.

[26] F. Fanelli, S. Lovascio, R. d'Agostino, F. Arefi-Khonsari, F. Fracassi, *Plasma Process. Polym.* **2010**, *7*, 535.

[27] J. H. Lee, T. T. T. Pham, Y. S. Kim, J. T. Lim, S. J. Kyung, G. Y. Yeom, *J. Electrochem. Soc.* **2008**, *155*, D163.

[28] L. J. Ward, W. C. E. Schofield, J. P. S. Badyal, A. J. Goodwin, P. J. Merlin, *Langmuir* **2003,** *19,* 2110.

[29] H. W. de Vries, E. Aldea, S. A. Starostin, M. Creatore, M. C. M. van de Sanden, Eur. Patent No. *2024533 A1*, **2009**.

[30] F. Fanelli, F. Fracassi, S. Lovascio, R. d'Agostino, *Contr. Plasma Phys.* **2011**, *51*, 137.

[31] NIST and Wiley libraries in *MassLab Release 1.4 (GC/MS Data System Software Finnigan)*.

[32] ACS Committee on Environmental Improvement, *Anal. Chem* **1980**, *52*, 2242.

Figure Captions

Figure 1. Schematic representation of the atmospheric pressure DBD reactor.

Figure 2. SEM images of coatings deposited in FDBDs fed with Ar, O_2 and different methyldisiloxanes : (a) O_2/HMDSO = 1, (b) O_2/HMDSO = 25, (c) O_2/HMDSO = 25 (downstream deposit), (d) O_2/PMDSO = 1, (e) O_2/PMDSO = 25, (f) O_2/PMDSO = 25 (downstream deposit), (g) O_2/TMDSO = 1, (h) O_2/TMDSO = 25, (i) O_2/TMDSO = 25 (downstream deposit).

Figure 3. Nomalized FT-IR spectra of thin films deposited by FDBDs fed by Ar, O_2 and different methyldisiloxanes (i.e., HMDSO and TMDSO) at the O_2/MDSO ratios in the feed of 0, 1 and 25.

Figure 4 FT-IR absorption integrals ratio Si-$(CH_3)_x$/Si-O-Si for HMDSO-, PMDSO- and TMDSO-containing DBDs as a function of the O_2/MDSO ratio in the feed.

Figure 5. (a) XPS carbon atomic percentage, (b) XPS O/Si ratio and (c) deposition rate obtained for HMDSO-, PMDSO- and TMDSO-containing DBDs as a function of the O_2/MDSO ratio in the feed.

Figure 6. Normalized FT-IR spectra of deposits obtained in the discharge zone (straight lines) and downstream the electrode region (dashed lines) with HMDSO, PMDSO and TMDSO at O_2/MDSO feed ratio of 25.

Figure 7. Normalized FT-IR spectra of coatings deposited in DBDs fed with Ar-MDSO-O_2 mixtures at O_2/MDSO feed ratio of 12, 10.5 and 9 for HMDSO, PMDSO and TMDSO, respectively.

Figure 8. GC-MS analyses exhaust gas of DBDs as a function of the O_2/MDSO feed ratio: (a) monomer depletion; (b) octamethyltrisiloxane trend for HMDSO- and PMDSO-fed plasmas; (c) trimethylsilanol trend for HMDSO- and PMDSO-fed DBDs; (d) hydroxypentamethyldisiloxane for HMDSO- and PMDSO-containing DBDs.

Figure 9. Possible pathways which could lead to the formation of some by-products (see Table 1) in HMDSO-containing DBDs considering the dissociation of both the Si-O (a) and Si-C (b) bonds in the precursor molecule.

Figure 10. General deposition mechanism scheme in organosilicon-containing atmospheric pressure DBDs.

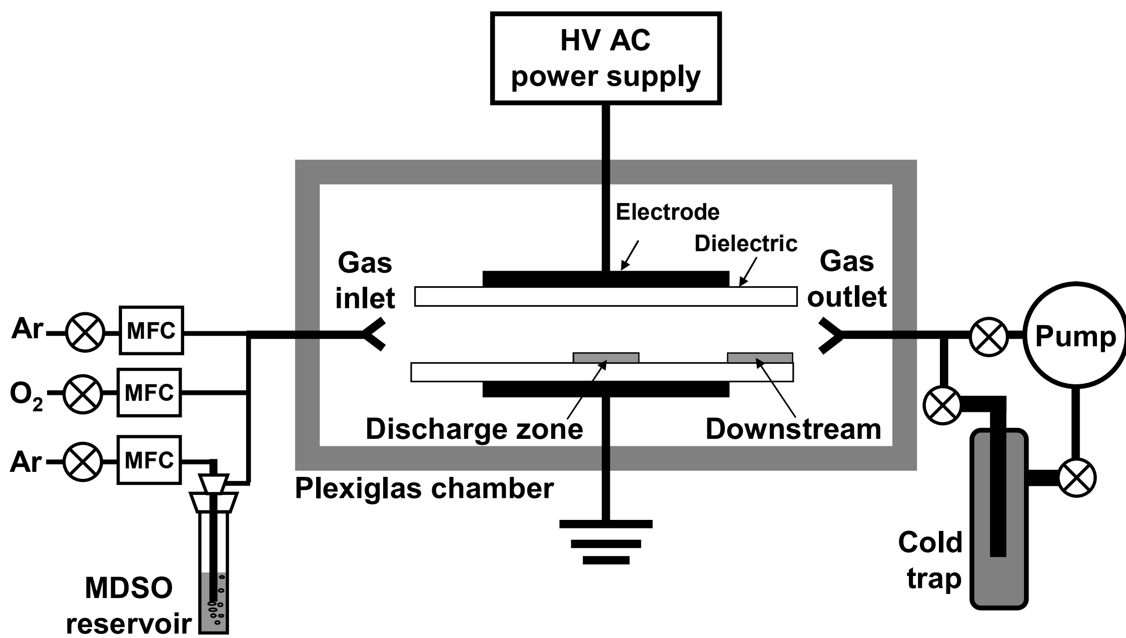

Figure 1. Schematic representation of the atmospheric pressure DBD reactor.

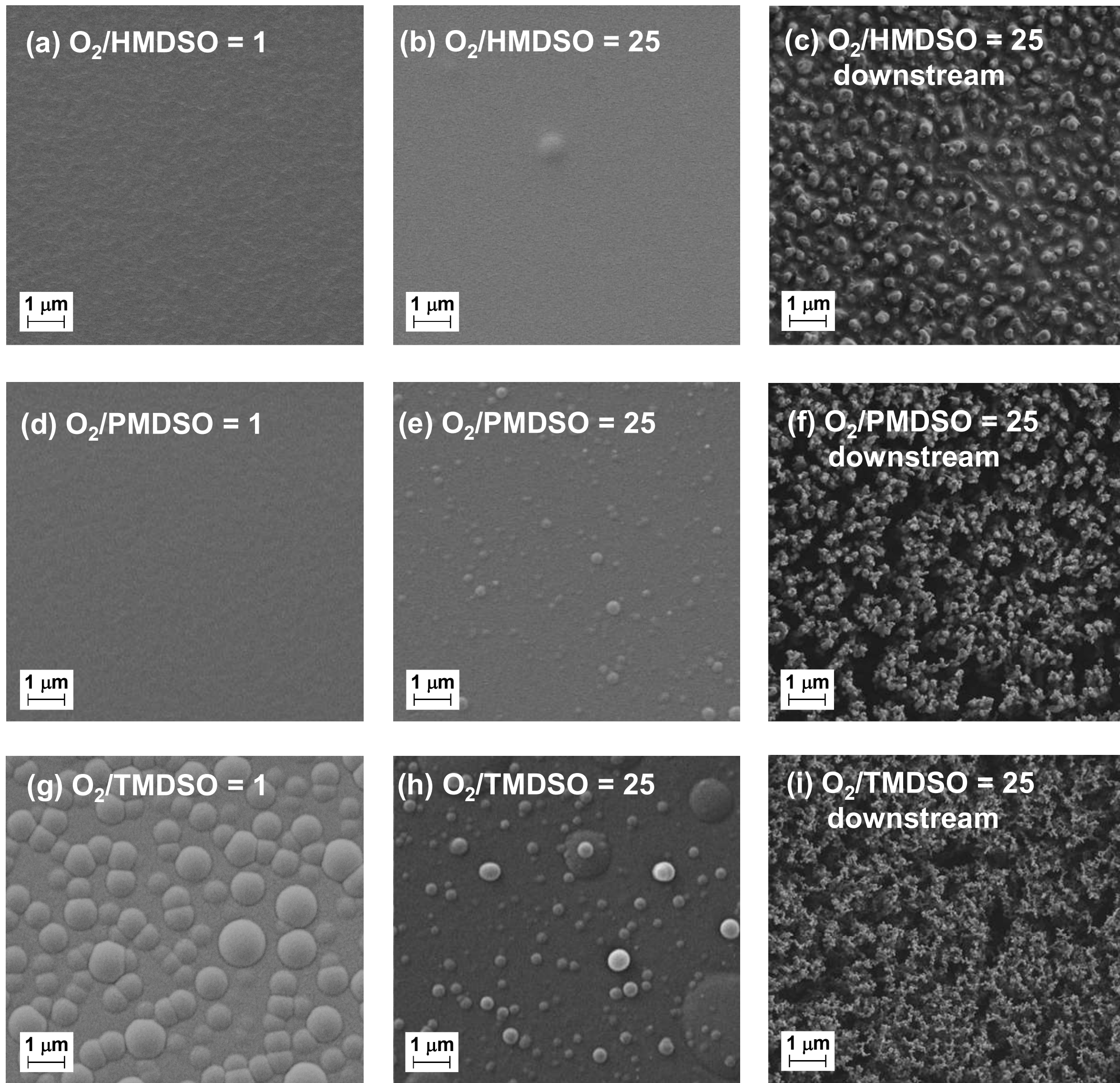

Figure 2. SEM images of coatings deposited in FDBDs fed by Ar, O_2 and different methyldisiloxanes : (a) O_2/HMDSO = 1, (b) O_2/HMDSO = 25, (c) O_2/HMDSO = 25 (downstream deposit), (d) O_2/PMDSO = 1, (e) O_2/PMDSO = 25, (f) O_2/PMDSO = 25 (downstream deposit), (g) O_2/TMDSO = 1, (h) O_2/TMDSO = 25, (i) O_2/TMDSO = 25 (downstream deposit).

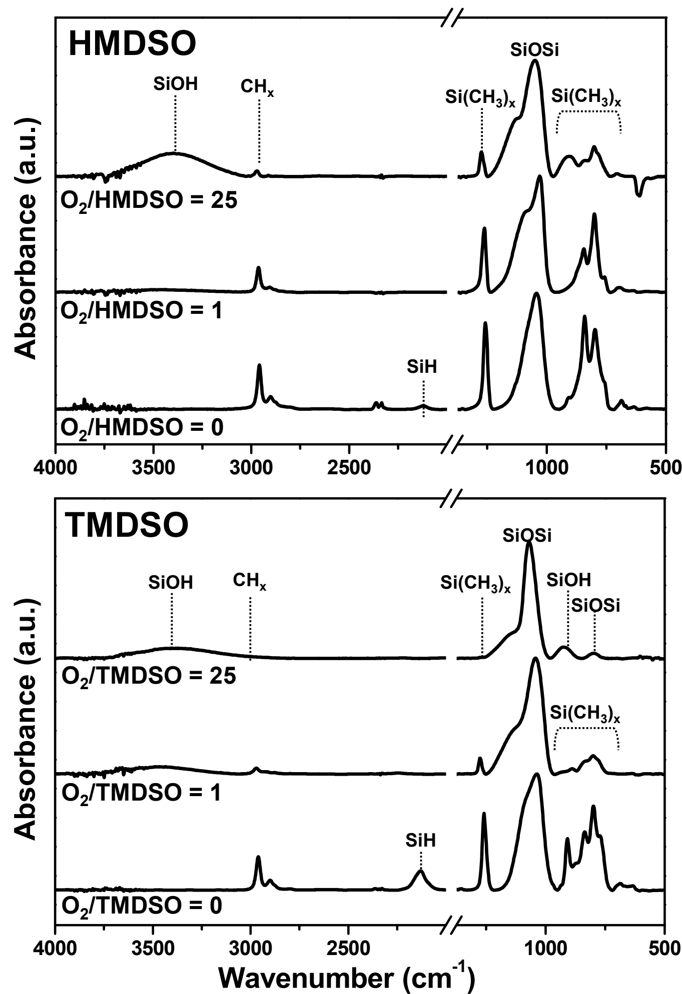

Figure 3. Nomalized FT-IR spectra of thin films deposited by FDBDs fed by Ar, O_2 and different methyldisiloxanes (i.e., HMDSO and TMDSO) at the O_2/MDSO ratios in the feed of 0, 1 and 25.

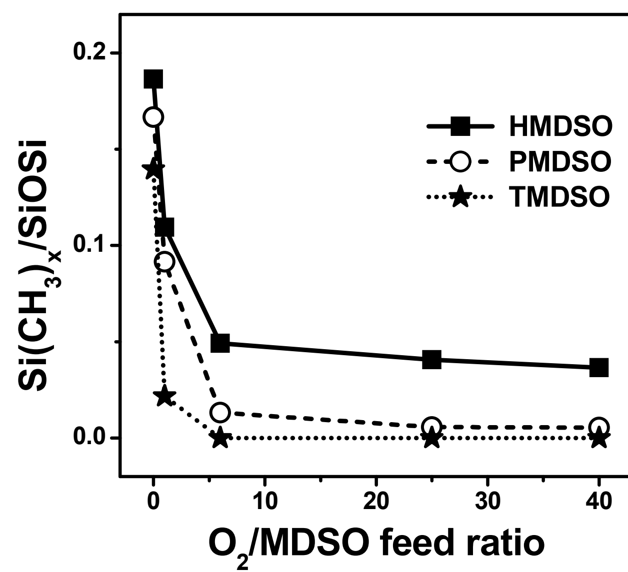

Figure 4. FT-IR absorption integrals ratio Si-$(CH_3)_x$/Si-O-Si for HMDSO-, PMDSO- and TMDSO-containing DBDs as a function of the O_2/MDSO ratio in the feed.

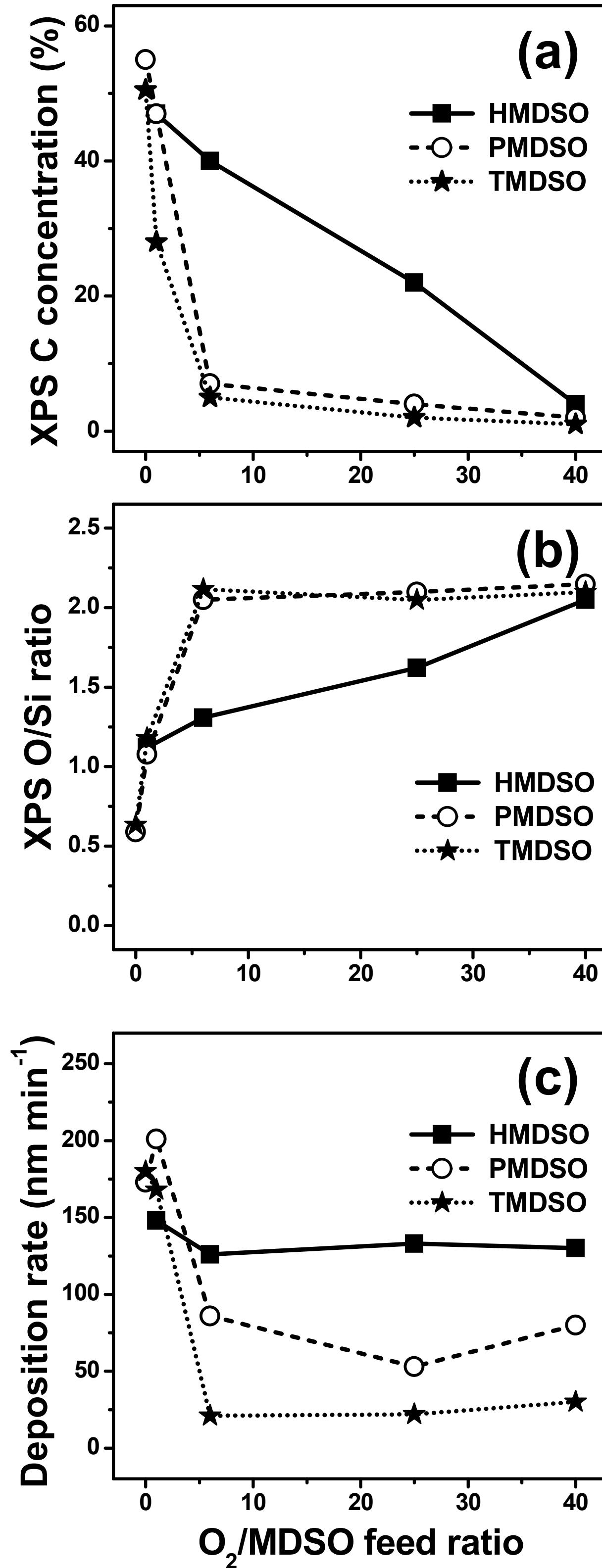

Figure 5. (a) XPS carbon atomic percentage, (b) XPS O/Si ratio and (c) deposition rate obtained for HMDSO-, PMDSO- and TMDSO-containing DBDs as a function of the O_2/MDSO ratio in the feed.

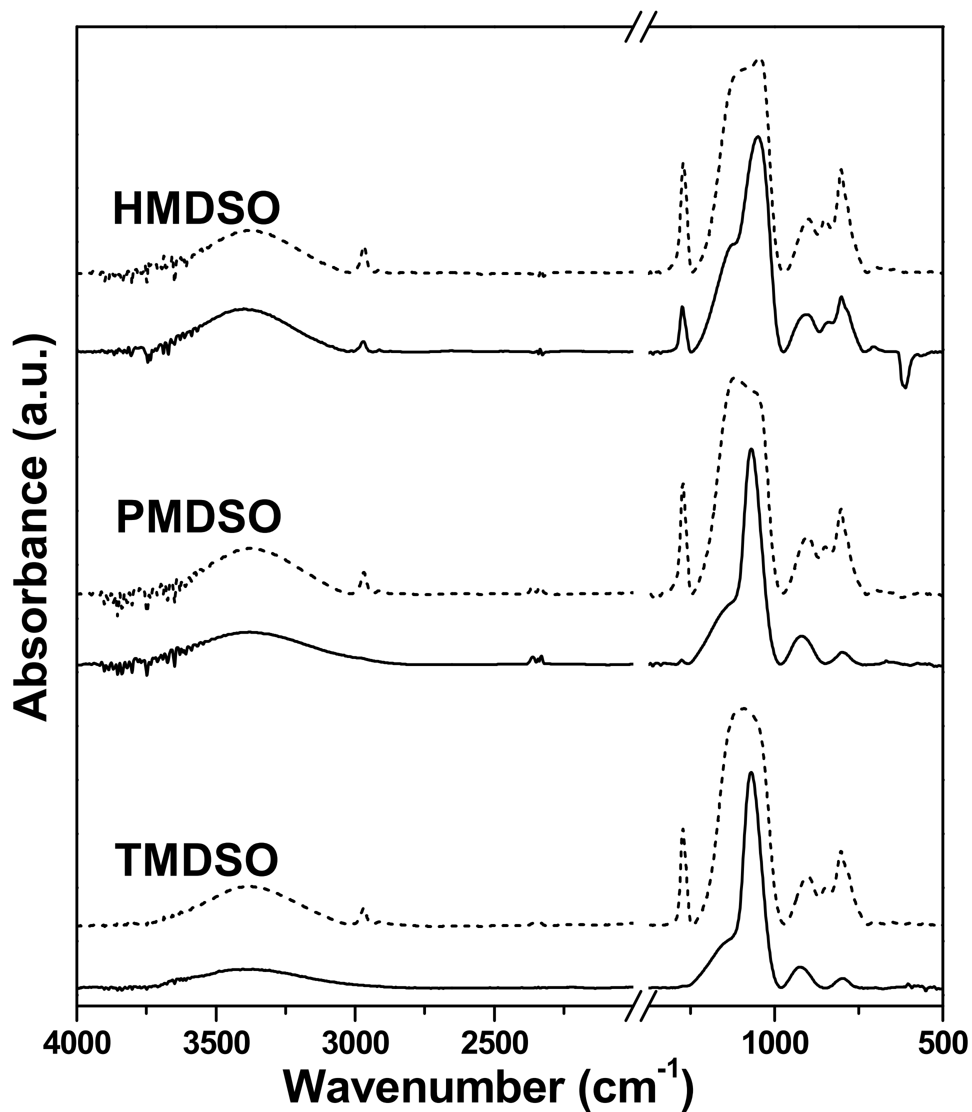

Figure 6. Normalized FT-IR spectra of deposits obtained in the discharge zone (straight lines) and downstream the electrode region (dashed lines) with HMDSO, PMDSO and TMDSO at O_2/MDSO feed ratio of 25.

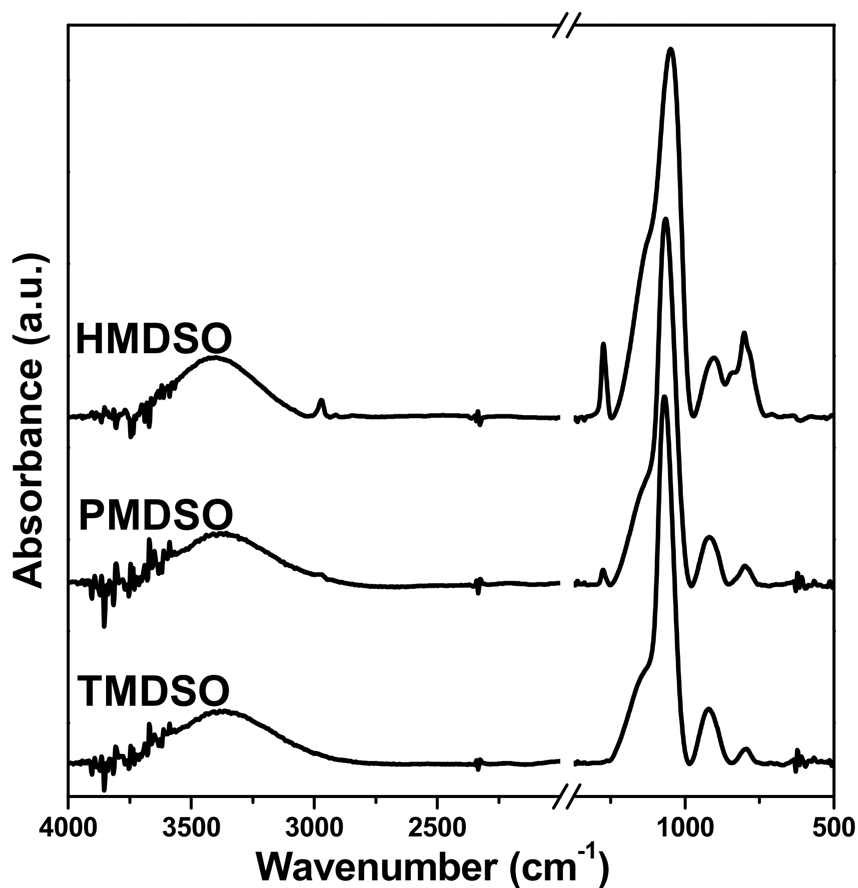

Figure 7. Normalized FT-IR spectra of coatings deposited in DBDs fed with Ar-MDSO-O_2 mixtures at O_2/MDSO feed ratio of 12, 10.5 and 9 for HMDSO, PMDSO and TMDSO, respectively.

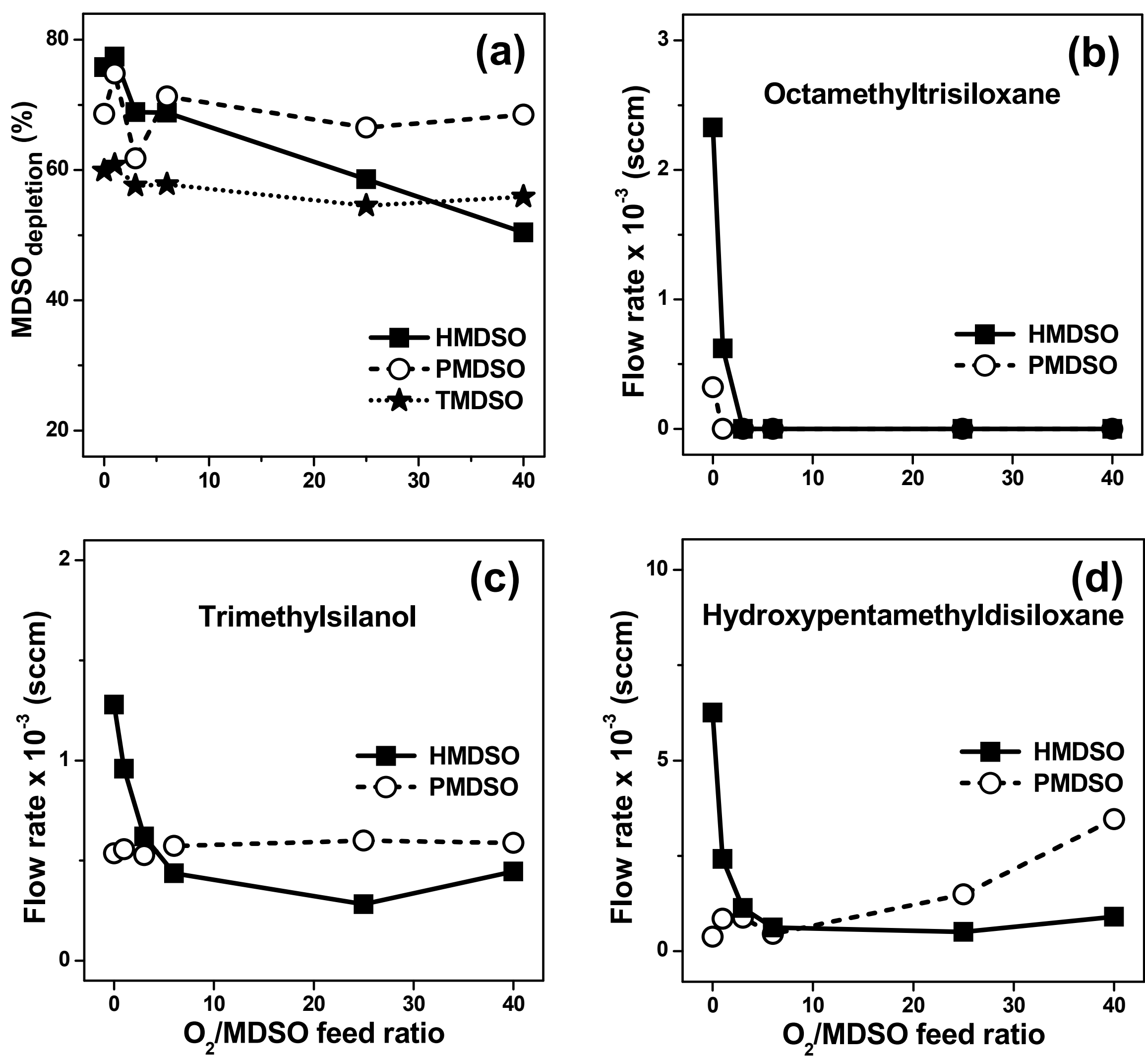

Figure 8. GC-MS analyses exhaust gas of DBDs as a function of the O_2/MDSO feed ratio: (a) monomer depletion; (b) octamethyltrisiloxane trend for HMDSO- and PMDSO-fed plasmas; (c) trimethylsilanol trend for HMDSO- and PMDSO-fed DBDs; (d) hydroxypentamethyldisiloxane for HMDSO- and PMDSO-containing DBDs.

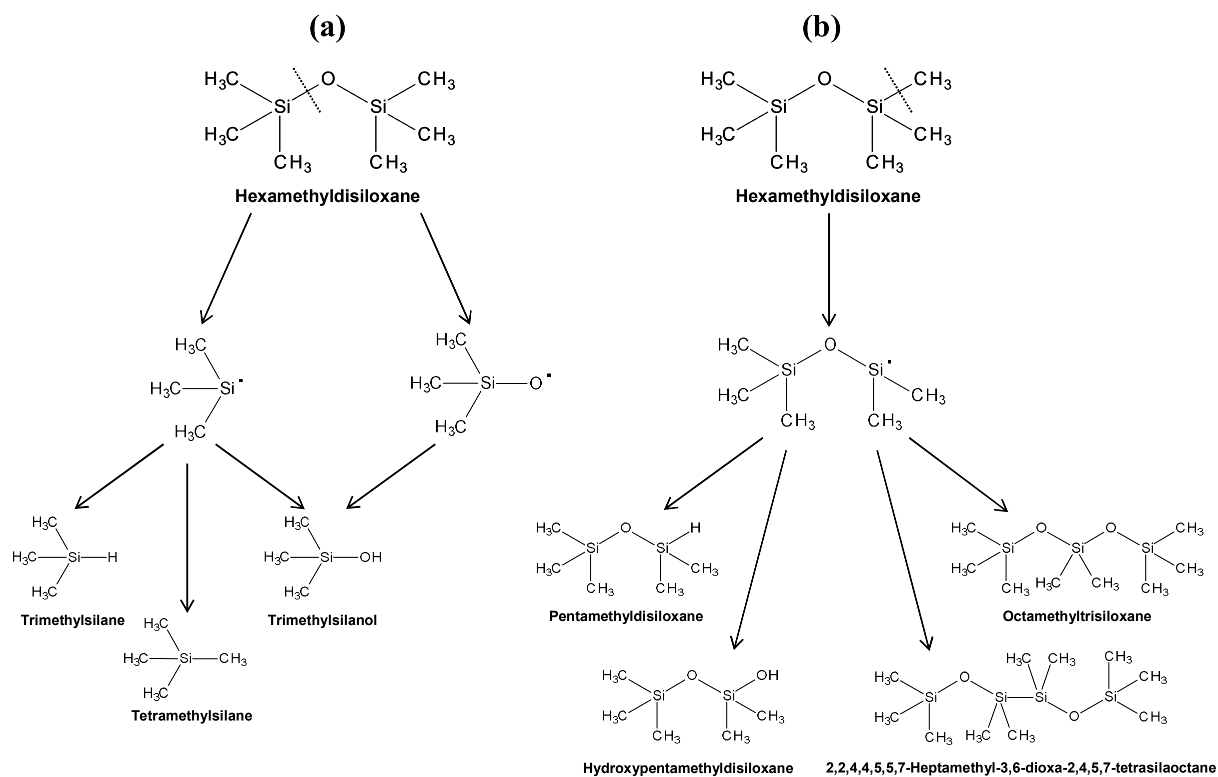

Figure 9. Possible pathways which could lead to the formation of some by-products (see Table 1) in HMDSO-containing DBDs considering the dissociation of both the Si-O (a) and Si-C (b) bonds in the precursor molecule.

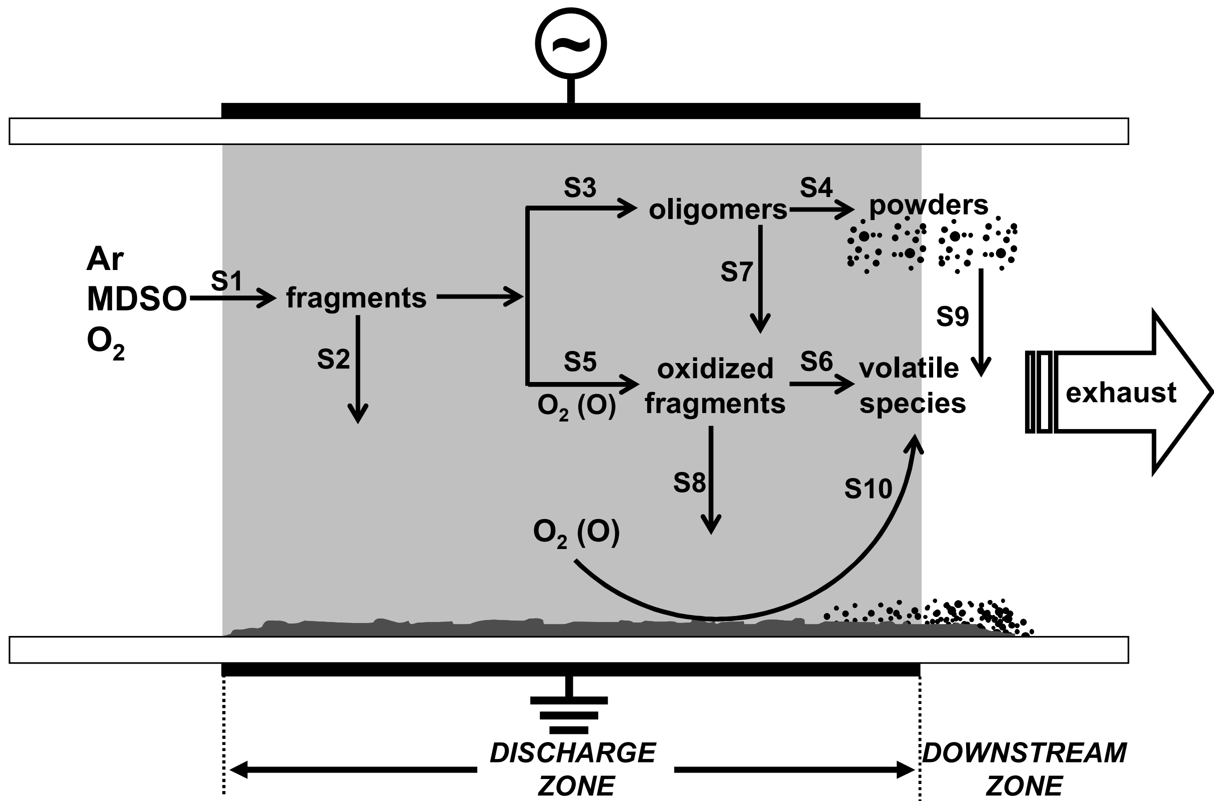

Figure 10. General deposition mechanism scheme in organosilicon-containing atmospheric pressure DBDs.

Table 1. Identified species detected in the exhaust gas of DBD fed by Ar-MDSO-O_2 mixtures.

	Compound	Formula	HMDSO	PMDSO	TMDSO
1	Trimethylsilane	$SiHMe_3$	✓	✓	✓
2	Tetramethylsilane	$SiMe_4$	✓	✓	✓
3	Ethyltrimethylsilane	$SiEtMe_3$	✓		
4	Trimethylsilanol	$SiMe_3OH$	✓	✓	
5	1,1,3,3-Tetramethyldisiloxane	$Me_2HSi\text{-}O\text{-}SiMe_2H$	✓	✓	✓
6	Pentamethyldisiloxane	$Me_3Si\text{-}O\text{-}SiMe_2H$	✓	✓	✓
7	Hexamethyldisiloxane	$Me_3Si\text{-}O\text{-}SiMe_3$	✓	✓	✓
8	Ethylpentamethyldisiloxane	$Me_3Si\text{-}O\text{-}SiEtMe_2$	✓		
9	Hydroxypentamethyldisiloxane	$Me_3Si\text{-}O\text{-}SiMe_2OH$	✓	✓	
10	1,1,3,3,5,5-Hexamethyltrisiloxane	$H\text{-}(Me_2SiO)_2\text{-}SiMe_2H$	✓	✓	✓
11	Hexamethylciclotrisiloxane	$(Me_2SiO)_3$	✓	✓	
12	1,1,1,3,5,5,5-Heptamethyltrisiloxane	$Me_3Si\text{-}O\text{-}SiMeH\text{-}O\text{-}SiMe_3$	✓	✓	
13	1,1,1,3,3,5,5-Heptamethyltrisiloxane	$Me\text{-}(Me_2SiO)_2\text{-}SiMe_2H$	✓	✓	
14	Octamethyltrisiloxane	$Me\text{-}(Me_2SiO)_2\text{-}SiMe_3$	✓	✓	
15	1-Ethyl-1,1,3,3,5,5,5-heptamethyltrisiloxane	$Et\text{-}(Me_2SiO)_2\text{-}SiMe_3$	✓		
16	3-Ethyl-1,1,1,3,5,5,5-heptamethyltrisiloxane	$Me_3Si\text{-}O\text{-}SiEtMe\text{-}O\text{-}SiMe_3$	✓		
17	Octamethylcyclotetrasiloxane	$(Me_2SiO)_4$	✓		
18	1,1,1,3,3,5,7,7,7-Nonamethyltetrasiloxane	$Me\text{-}(Me_2SiO)_2\text{-}SiMeH\text{-}O\text{-}SiMe_3$	✓		
19	1,1,1,3,3,5,5,7,7-Nonamethyltetrasiloxane	$Me\text{-}(Me_2SiO)_3\text{-}SiMe_2H$	✓		
20	Decamethyltetrasiloxane	$Me\text{-}(Me_2SiO)_3\text{-}SiMe_3$	✓		
21	2,2,4,4,5,5,7-Heptamethyl-3,6-dioxa-2,4,5,7-tetrasilaoctane	$Me_3Si\text{-}O\text{-}SiMe_2\text{-}SiMe_2\text{-}O\text{-}SiHMe_2$		✓	
22	2,2,4,4,5,5,7,7-Octamethyl-3,6-dioxa-2,4,5,7-tetrasilaoctane	$Me_3Si\text{-}O\text{-}SiMe_2\text{-}SiMe_2\text{-}O\text{-}SiMe_3$	✓	✓	
23	Dodecamethylpentasiloxane	$Me\text{-}(Me_2SiO)_4\text{-}SiMe_3$	✓		

This work deals with the atmospheric pressure PE-CVD of thin films using DBDs fed with argon, oxygen and different methyldisiloxanes. Results form the investigation of the chemical composition and structure of the deposits, as well as from the qualitative and quantitative analysis of the exhaust gas, are exploited to rise hypotheses on the overall deposition mechanism and on the organosilicon plasma chemistry at atmospheric pressure.

F. Fanelli,* S. Lovascio, R. d'Agostino, F. Fracassi

Insights into the Atmospheric Pressure Plasma-Enhanced Chemical Vapor Deposition of Thin Films from Methyldisiloxane Precursors